Available online at www.sciencedirect.com
ScienceDirect
Biochimica et Biophysica Acta 1768 (2007) 2263–2270
Biochimica et Biophysica Acta
BBA
www.elsevier.com/locate/bbamem

Segment TM7 from the cytoplasmic hemi-channel from V_O-H^+-V-ATPase includes a flexible region that has a potential role in proton translocation ☆

Afonso M.S. Duarte [a], Edwin R. de Jong [a], Rainer Wechselberger [c], Carlo P.M. van Mierlo [b], Marcus A. Hemminga [a,*]

[a] *Laboratory of Biophysics, Wageningen University, Dreijenlaan 3, 6703 HA Wageningen, The Netherlands*
[b] *Laboratory of Biochemistry, Wageningen University, The Netherlands*
[c] *Department of NMR Spectroscopy, Bijvoet Centre for Biomolecular Research, Utrecht University, The Netherlands*

Received 23 January 2007; received in revised form 23 April 2007; accepted 11 May 2007
Available online 21 May 2007

Abstract

A 900-MHz NMR study is reported of peptide sMTM7 that mimics the cytoplasmic proton hemi-channel domain of the seventh transmembrane segment (TM7) from subunit *a* of H^+-V-ATPase from *Saccharomyces cerevisiae*. The peptide encompasses the amino acid residues known to actively participate in proton translocation. In addition, peptide sMTM7 contains the amino acid residues that upon mutation cause V-ATPase to become resistant against the inhibitor bafilomycin. 2D TOCSY and NOESY ^1H–^1H NMR spectra are obtained of sMTM7 dissolved in d_6-DMSO and are used to calculate the three-dimensional structure of the peptide. The NMR-based structures and corresponding dynamical features of peptide sMTM7 show that sMTM7 is composed of two α-helical regions. These regions are separated by a flexible hinge of two residues. The hinge acts as a ball-and-joint socket and both helical segments move independently with respect to one another. This movement in TM7 is suggested to cause the opening and closing of the cytoplasmic proton hemi-channel and enables proton translocation.

Keywords: NMR; Transmembrane; V-ATPase subunit *a*; Peptide conformation; Proton translocation

1. Introduction

One of the most important balances required for cell maintenance and activity is the establishment of differences in pH between various cellular organelles. This balance is mainly provided by vacuolar proton ATPases (V-ATPases)[1], which act as molecular motors that pump protons across a membrane. Proton translocation occurs at the expense of ATP that is hydrolyzed in the V_1 catalytic cytoplasmic domain of V-ATPase. The protons involved pass the membrane through the transmembrane V_O domain. This domain contains subunits *a*, *d*, *e*, which are part of the stator of the molecular motor, and proteolipid subunits *c*, *c′* and *c″* (*c*-subunits) that make up the rotor [1].

V-ATPases reside in membranes of vacuoles, endosomes and lysosomes and cause the acidification of theses compartments [2,3]. In specific cases V-ATPase is present in the cell membrane causing the acidification of the extracellular space. Such extracellular acidification happens in the case of osteoclasts, which are a particular type of bone cells. In osteoclasts deregulation of H^+-V-ATPase can lead to bone demineralization leading to osteoporosis. Although several drugs are available to reduce bone loss they only have a temporary effect. One factor that impedes the discovery of new

Abbreviations: CSI, Chemical shift index; DMSO, Dimethylsulfoxide; DSS, Sodium 2,2-dimethyl-2-silapentane-5-sulfonate; HMBC, Heteronuclear multiple bond correlation; HSQC, Heteronuclear single quantum coherence; sMTM7, Peptide mimicking the cytoplasmic side of the seventh transmembrane segment of subunit *a* from V-ATPase; NMR, Nuclear magnetic resonance; NOESY, Nuclear Overhauser enhancement spectroscopy; TM, Transmembrane; RMSD, Root-mean-square deviation; TOCSY, Total correlation spectroscopy; V-ATPase, Vacuolar proton-translocating adenosine triphosphatase; SA, simulated annealing

☆ The final high resolution structures and the NMR data were deposited with the following references: PDB databank—2NVJ; BioMagResbank BMRB—15025.

* Corresponding author. Tel.: +31 317 482 635; fax: +31 317 482 725.
E-mail address: marcus.hemminga@wur.nl (M.A. Hemminga).
URL: http://ntmf.mf.wau.nl/hemminga/ (M.A. Hemminga).

0005-2736/$ - see front matter © 2007 Elsevier B.V. All rights reserved.
doi:10.1016/j.bbamem.2007.05.014

therapies is the lack of high-resolution structural and dynamical information about the V_O domain of V-ATPase. The structure of the rotor subunits has recently been elucidated for a related enzyme, the Na^+-V-ATPase [4]. However, no high-resolution structure is available for the stator subunits. Recently, our group experimentally demonstrated [5,6] that the seventh transmembrane segment (TM7) of the stator subunit *a* of V-ATPase possesses α-helical properties. However, no structure at atomic resolution could be obtained. Interest in the three-dimensional structure and chemical and physical properties of TM7 is high as several of its residues were shown to be involved in the binding of inhibitors of V-ATPase [7].

Subunit *a* of V-ATPase is composed of nine putative transmembrane sections and a 400-residue cytoplasmic section [8,9]. Residue R735 of TM7 plays a vital role since its mutation provokes total inhibition of proton translocation [8]. Mutating histidine residues H729 and H743 of TM7 also affects proton translocation, although their effect is less pronounced compared to the mutations of R735.

Proteolipid rotor subunits *c*, *c′* and *c″* are transmembrane subunits also involved in proton translocation. They are composed of four TM segments and *c″* has an additional fifth cytoplasmic segment. The glutamic acid residues of the fourth putative TM segment of *c* and *c′*, and of the second putative transmembrane segment of *c″* are of fundamental importance for proton translocation [2,9,10]. Two hemi-channels provide a proposed pathway that protons can follow during their translocation [11]. It is assumed that rotation of the rotor, which is due to hydrolysis of ATP in the V_1 domain, forces protonation of the glutamic acid residues mentioned. Protons can access the carboxylic side chain of these residues via a cytoplasmic hemi-channel that is located in the interface between subunit *a* and the rotor. When a *c*-subunit rotates the release of another proton into the luminal hemi-channel occurs. This release is assisted by R735 of TM7 as it stabilizes the negatively charged side chain of the glutamic acid involved.

The cytoplasmic hemi-channel acts as a binding pocket for bafilomycin [7] and the potential residues involved are located at the interface between TM4 (of the rotor) and TM7 (of subunit *a*). During proton translocation the relative orientation of these two helical segments changes due to rotation of one or of both helical segments [12]. Inhibition of proton translocation occurs when these two segments are constrained to one rigid conformation that prohibits the swiveling of the glutamic acid located in the centre of the rotor [13].

Here, a 900-MHz NMR study is reported of peptide sMTM7 (Fig. 1) that mimics the cytoplasmic proton hemi-channel domain of TM7 from the yeast *Saccharomyces cerevisiae*. Peptide sMTM7 is a shorter version of peptide MTM7 that we studied previously [5], but still encompasses the amino acid residues known to actively participate in the cytoplasmic proton translocation hemi-channel (i.e., H729, R735, H743). In addition, peptide sMTM7 contains the amino acid residues that upon substitution cause V-ATPase to become resistant against bafilomycin (i.e., residues E721, L724 and N725) [7]. The use of a shortened version of MTM7 leads to 2D ^1H–^1H NMR spectra of sufficient quality to extract NOE constrains and calculate the three-dimensional structure of the peptide at atomic resolution. The NMR-based structures of peptide sMTM7 provide new insight in the involvement of TM7 of subunit *a* in proton translocation.

2. Materials and methods

2.1. Peptide design and synthesis

The 25-residue peptide sMTM7 was designed (Fig. 1) based on the putative localization of MTM7 in the cytoplasmic hemi-channel [5,7,9]. Throughout this paper the sequential numbering of amino acid residues of peptide sMTM7 is identical to the one used for subunit *a* in V-ATPase (Fig. 1). Peptide sMTM7 was produced on solid support using continuous flow chemistry by Pepceuticals Ltd., Leicester, UK. Its purity was tested by mass spectrometry and found to be larger than 90%.

2.2. NMR measurements

Peptide sMTM7 is a highly hydrophobic peptide with a low solubility in aqueous systems. Different membrane-mimicking solvents were tested, however, only the use of DMSO avoided aggregation at peptide concentrations needed for NMR spectroscopy (data not shown). Consequently, DMSO was used to obtain 2D ^1H–^1H NMR and natural abundance 2D ^1H–^{13}C spectra of peptide sMTM7 with sufficient signal-to-noise ratio.

NMR samples were made by dissolving peptide sMTM7 in 500 μL d_6-DMSO (Cambridge Isotopes) to a concentration of 2 mM. DSS (Cambridge Isotopes) was used as internal standard. ^1H and natural abundance ^{13}C NMR spectra were recorded at 900 MHz on a Bruker DRX900 spectrometer. 2D ^1H–^1H-NOESY, ^1H–^1H-TOCSY, and natural abundance 2D ^1H–^{13}C HSQC and HMBC spectra were recorded according to Ref. [14]. All spectra were recorded at 30 °C. 2D NOESY experiments were acquired with mixing times of 100, 200, and 300 ms. 2D TOCSY experiments were acquired with a mixing time of 70 ms. In case of all 2D-NMR experiments 2K data points were collected in the

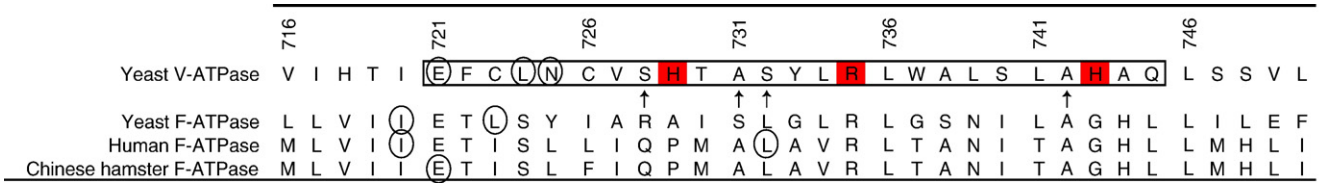

Fig. 1. Amino acid alignment of the TM7 segment of V-ATPase subunit *a* of yeast with the equivalent TM segment of subunit *a* from F-ATPase (i.e., TM4) from yeast, human and Chinese hamster, respectively. Activity related-amino acid residues of TM7 from yeast V-ATPase are shown in red (H729, R735 and H743). Peptide sMTM7 is indicated by a horizontal box. Amino acid residues that upon substitution cause V- and F-ATPase to become resistant against bafilomycin are shown by circles [7]. Arrows show the amino acid residues that strongly cross link with the proteolipid subunits *c′* and *c″* [12,13]. Amino acid numbering is based on the sequence of full-length subunit *a*.

t_2 dimension and 1K data points were collected in the t_1 dimension. The spectral width was 11 ppm for ^{1}H and 140 ppm for ^{13}C for both 2D ^{1}H–^{13}C HMBC and HSQC. NMR data were processed using XWINNMR from Bruker. Peak assignment and spectral analysis were carried out using the software Sparky (Goddard, T. D., and Kneller, D. G., University of California, San Francisco) running under Linux.

2.3. Structure calculations

The software package CNS[15] combined with the ARIA 1.2 setup and protocols[16,17] was used to calculate structures of peptide sMTM7 that are consistent with the obtained NMR data. As input for the structure determination and refinement ambiguously and unambiguously identified NOE contacts were used. A simulated annealing protocol in Cartesian space was employed. The protocol starts with an extended conformation of peptide sMTM7 and involves four stages: (a) simulated annealing stage at 2000 K (10000 steps); (b) first cooling phase to 1000 K in 5000 steps; (c) second cooling stage to 50 K in 2000 steps; (d) final 200 steps of energy minimization. The time step for integration was set to 0.003 ps. The resulting structures were subjected to a final refinement by solvation with DMSO. A total of 160 structures were calculated and out of these 20 structures that have the lowest energies were selected. The RMSD calculations and superimposition were performed with the software package MOLMOL [18].

3. Results

3.1. Assignment of NMR resonances of sMTM7 in d_6-DMSO

2D ^{1}H–^{1}H TOCSY, ^{1}H–^{1}H NOESY and natural abundance ^{1}H–^{13}C HSQC and HMBC spectra are recorded of peptide sMTM7 in d_6-DMSO. Assignment of its spin systems is based on the technique of sequential resonance assignments[19,20] by making interactive interpretations of the 2D ^{1}H–^{1}H TOCSY and 2D ^{1}H–^{1}H NOESY spectra. Fig. 2 shows the ^1H_N–$^1H_\alpha$ and ^1H_N–^1H_N regions of the 300-ms NOESY spectrum of sMTM7. The resonance assignments are provided in Table 1 of the Supplemental Data and are deposited, together with the NOESY assignments, in the BioMagResbank under access number 15025.

The ^{13}C spectra provide information that facilitates the assignment procedure. In addition, the chemical shifts of $^{13}C_\beta$ of C723 (38.254 ppm) and of C726 (36.953 ppm) report about the oxidative state of the cysteine residues. As the $^{13}C_\beta$ chemical shift of reduced cysteines fall in the region 24–33 ppm and those of oxidized cysteines in the region 34–52 ppm [21,22] it is concluded that C723 and C728 are involved in a disulphide bond. No inter-molecular cross-links between sMTM7 molecules are identified in the 2D-NOESY spectra. Consequently, C723 and C726 are linked by an intramolecular disulphide bond and sMTM7 is monomeric.

3.2. Secondary structure

The chemical shift index (CSI)[23] is calculated for the $^1H_\alpha$ protons of sMTM7 (Fig. 3). Many residues have a propensity to be in an α-helix configuration as is inferred from consecutive negative $^1H_\alpha$ CSI values, with residues V727, L734 and L736 being exceptions.

The observation of specific sequential and medium-range NOE contacts can be used to infer the secondary structure of peptides and proteins [19,20]. The NOE connectivities relevant to do the latter for peptide sMTM7 (i.e., $d_{\alpha N}(i, i+3)$, $d_{\alpha N}(i, i+4)$ and $d_{\alpha N}(i, i+5)$ connectivities) are shown in Fig. 3. A helical region exists between C723 and A738 as suggested by many NOEs (seven $d_{\alpha N(i,i+3)}$, eight $d_{\alpha N(i,i+4)}$ and three $d_{\alpha N(i,i+5)}$ connectivities) and its presence is supported by the CSI data. The absence of $d_{\alpha N}(i,i+4)$ and $d_{\alpha N}(i,i+5)$ NOE contacts in the region T730–A731 suggests that the helical segment might be disrupted. In the region A738–Q745 only one $d_{\alpha N(i,i+4)}$ NOE contact is found, which suggests that this part of the peptide does not adopt a helical conformation.

3.3. Structure calculations

A number of 545 distance constraints extracted from the ^{1}H–^{1}H-NOESY spectrum of peptide sMTM7 are used as input for the structure calculation procedure. These constraints include the NOE contacts shown in Fig. 3, as well as medium- and long-range NOE contacts identified between side chains of different amino acid residues. The conformational properties of the resulting 20 lowest energy struc-

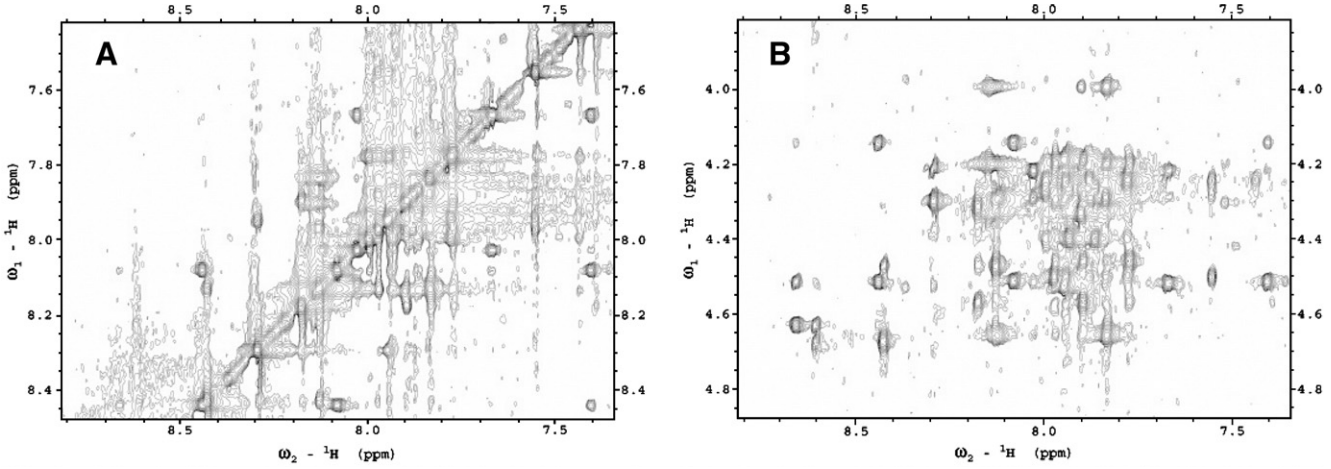

Fig. 2. Fingerprint ^1H_N–^1H_N (A) and ^1H_N–$^1H_\alpha$ (B) regions of the 900-MHz 2D-NOESY spectrum of peptide sMTM7 in d_6-DMSO at 30 °C (mixing time of 300 ms).

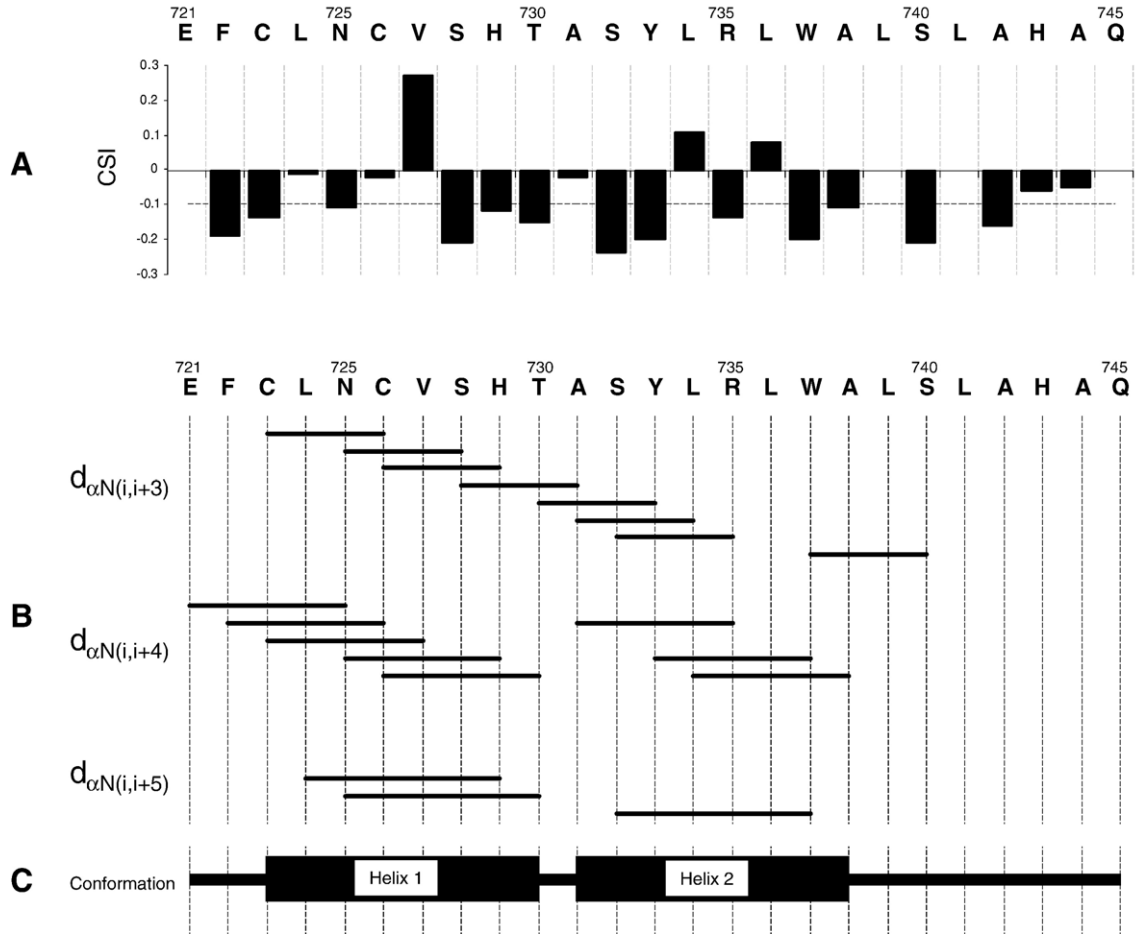

Fig. 3. Summary of several secondary structure data obtained for peptide sMTM7 in d_6-DMSO at 30 °C. (A) Chemical Shift Index for $^1H_\alpha$ (■), residues with CSI values that lie below −0.1 (----) have a high probability to be in an α-helical conformation. (B) NOE connectivities $d_{\alpha N}(i, i+3)$, $d_{\alpha N}(i, i+4)$ and $d_{\alpha N}(i, i+5)$. C: Secondary structure within peptide sMTM7 as deduced from NOEs and from the simulated annealing approach that leads to structures at atomic resolution.

tures of peptide sMTM7 in d_6-DMSO are shown in Fig. 4. These structures are deposited in the PDB databank with reference 2NVJ. Fig. 5 depicts the ribbon drawings of these structures. Fig. 4 shows that several regions of peptide sMTM7 are able to adopt different secondary structures. For example region S732–R735 adopts an α-helical conformation in ten structures, a 3_{10}-helix in three structures and turn/bend conformations in seven of the 20 lowest energy structures calculated.

Taking into account the conformations obtained from the structure calculations (Fig. 4), two main regions in peptide sMTM7 that populate helical conformations are identified: C723–H729 and S732–A738. RMSD minimization fits of three different regions of the backbone of the 20 lowest energy structures calculated are shown in Fig. 6. The superimposition of the structures confined to either of the two identified helical regions (C723–H729 and S732–A738) leads to relatively low RMSD values thereby confirming the helical character of both sections of sMTM7. These two helical regions act as separate moieties that move independently with respect to one another due to the less rigid section involving T730–A731 (Fig. 6A and B). The existence of such a flexible region is confirmed by the identification of weak long-distance NOE contacts between the side chains of residues located in Helix 1 and Helix 2 (for example, a NOE contact is found between the sidechains of E721 and Q745). These NOE contacts are included in the structure determination procedure (all NOE contacts have been deposited in the BioMagResbank). A RMSD minimization of the region T730–A731 (Fig. 6C) shows that both helical regions move independently with respect to one another. The region L-739–Q745 of sMTM7 is fraying.

4. Discussion

To study the intrinsic conformational properties of the putative cytoplasmic hemi-channel region of TM7 of V-ATPase subunit *a* a 25-residue peptide sMTM7 was designed as a mimic of TM7. The putative TM7 has α-helical character in different membrane-mimicking solvents (SDS, DMSO, TFE and lipid bilayers) [5,6,24]. However, no three-dimensional structure at atomic resolution is available for TM7. Here the

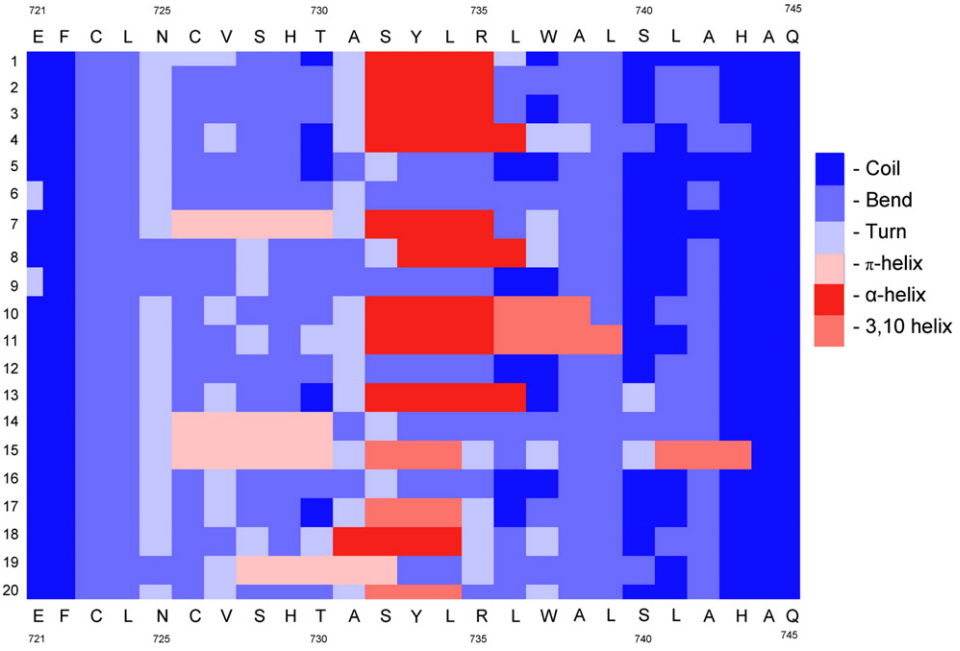

Fig. 4. Matrix representation of the conformational properties of the 20 lowest energy structures of peptide sMTM7 as determined by the ARIA software. The horizontal axis represents the sequence of peptide sMTM7 and the vertical axis shows the corresponding secondary structure element in each of the structures calculated.

NMR-based 3D structures of sMTM7 are reported and as a result new insight in the involvement of TM7 in proton translocation is obtained.

Recently, ESR spectroscopy and Molecular Dynamics simulations suggested that peptide sMTM7 adopts α-helical conformation in SDS micelles [6]. The 2D $^{1}H-^{1}H$-NMR studies reported here require much higher concentrations of peptide sMTM7 as compared to what is needed in the ESR studies [6]. DMSO is commonly used as an appropriate solvent to study the structure and dynamics of various membrane peptides [5,25–28]. DMSO indeed allows the use of the high sMTM7 concentrations (i.e., 2 mM) needed to obtain high-resolution 2D $^{1}H-^{1}H$ NMR spectra of sufficient quality. Other solvents have been tested as well, but the solubility of peptide sMTM7 is either too low or the obtained signal-to-noise ratio is too poor. The three-dimensional structure and dynamics of peptide sMTM7 in DMSO are determined by using NMR spectroscopy at 900 MHz to obtain good sensitivity and dispersion of the resonances involved. All spin systems (i.e., amino acid residues) are assigned in the TOCSY spectrum and 80% of the NOEs observed could be unambiguously assigned in the NOESY spectra.

The combination of CSI values and NOE contacts (Fig. 3) indicates that peptide sMTM7 predominantly adopts an α-helical structure in the region between C723 and A738. The identification of three $d_{\alpha N(i,i+5)}$ contacts (L724–H729, N725–T730 and S732–W737) suggest that in these regions of the peptide a conformational exchange between α-helical and more loosened helical conformation occurs (π-helical).

The 20 lowest energy structures derived for peptide sMTM7 (Figs. 4 and 5) show that the peptide is composed

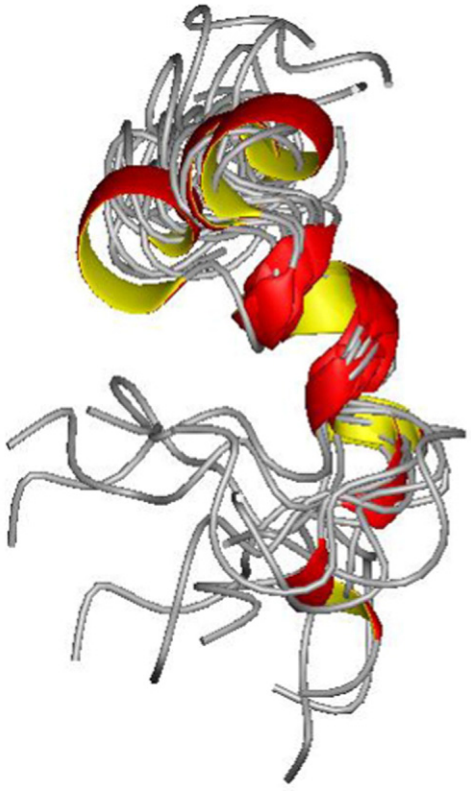

Fig. 5. Ribbon representations of the conformations of the 20 lowest energy structures determined of peptide sMTM7 in d_6-DMSO. Structures are drawn with the software package MOLMOL [18]. These structures are deposited in the PDB databank with reference 2NVJ.

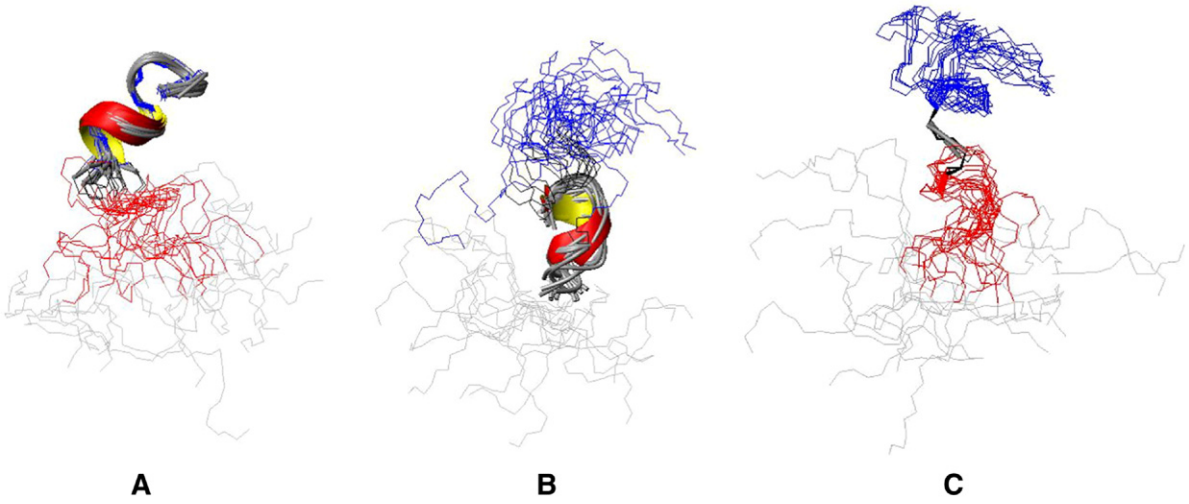

Fig. 6. Three RMSD-minimized superposition of the C_α traces of the 20 lowest energy structures calculated for peptide sMTM7 using the software MOLMOL [18]. The RMSD is minimized for the following three regions of the peptide: (A) residues C723–H729 (RMSD: 1.130 Å), (B) residues S732–A738 (RMSD: 3.212 Å), and (C) residues T730–A731 (RMSD: 0.890 Å). The regions with RMSD-minimization are depicted in the ribbon representation, the remaining sections are depicted in their C_α traces. The four regions identified in sMTM7 are differently colored for the purpose of distinction: blue—E721–H729, black—T730–A731, red—S732–A738 and dark grey—A738–Q745.

of two α-helical regions: C726–H729 and S732–A738. These two helical segments are separated by a region (T730–A731) in which coil/bend/turn conformations are predominantly populated (see Fig. 4). In the C-terminal part of peptide sMTM7 no medium nor long-range NOEs are detected between residues A738 and Q745 and as a conse-

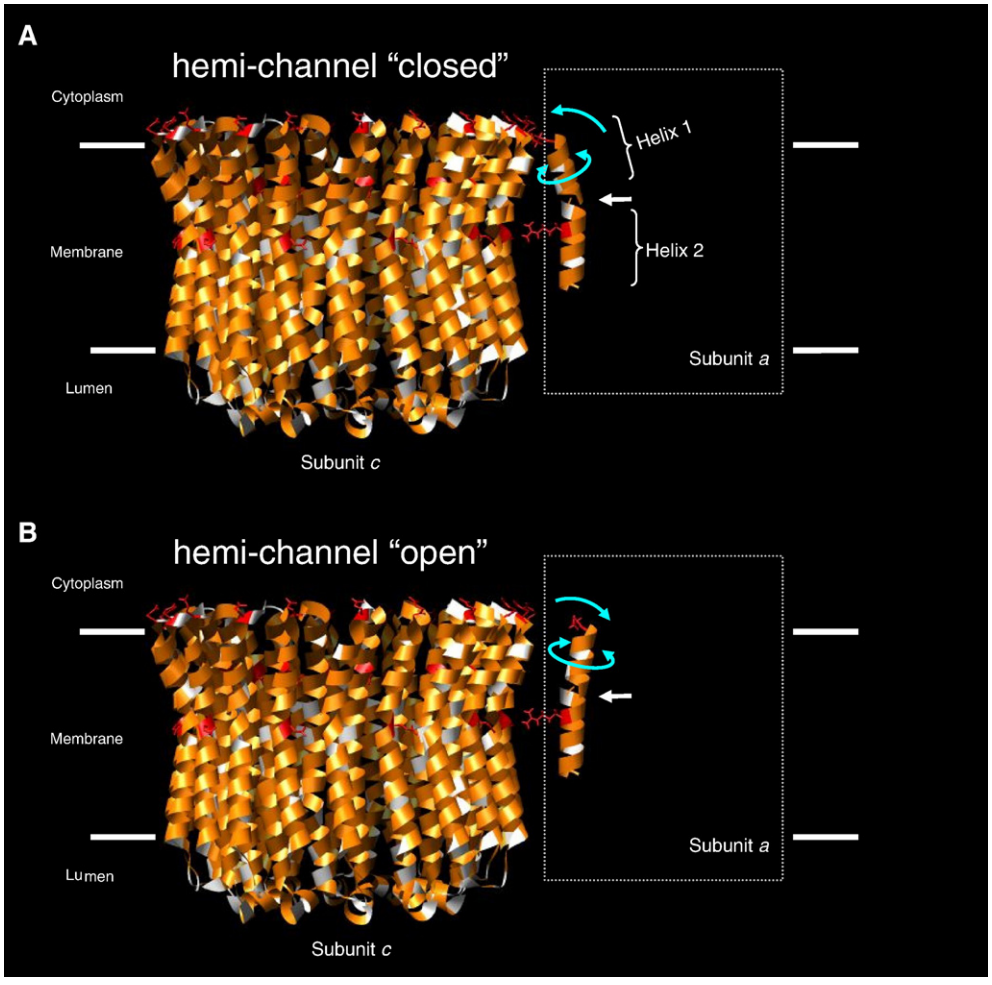

quence the structure calculations show that this section mainly populates coil/bend/turn conformations, which reflects conformational fraying. C-termini of peptides have stronger fraying properties than N-termini [29,30]. In case of sMTM7 the disulphide bridge that links C723 and C726 contributes to the virtual absence of fraying of the N-terminus (Fig. 6A). The first helical segment of sMTM7 is apparently dynamic as it can adopt turn, bend and π-helical conformations and resembles a loosened α-helix (Figs. 4–6). The second helical segment of sMTM7 adopts α-helical and 3_{10}-helical conformations. This part of sMTM7 is less dynamic compared to the first helical section as turn and bend structures are hardly populated. Both helical segments are connected by two amino acid residues (T730 and A731) that adopt turn and bend conformations (Fig. 4). As a result, both helical segments move independently with respect to one another (Fig. 6).

Previous NMR studies in which a 12-residue longer version of peptide sMTM7 was used [5] postulate that the C723–A731 region is helical. However, on the basis of the previous data which lack assignments due to the size of the molecule investigated and in which NOEs are only qualitatively interpreted, it could not be excluded that this helical segments contains small non-helical segments. The refined study presented here indeed shows that TM7 does not adopt a continuous α-helical structure, but instead it has a flexible non-helical hinge region at T730–A731. A recent study from Underhaug [31] identified a flexible region in a peptide from the Na^+,K^+-ATPase that was correlated with a flexible region in the native protein. Backbone hinges that interrupt transmembrane helical segments have been identified for other transmembrane protein [32].

The conformational characteristics observed for peptide sMTM7 reflect the intrinsic proprieties of the peptide. Consequently, it is proposed that the sMTM7 part of TM7 exhibits similar behavior when it is located in its natural environment, subunit *a* of V-ATPase. How might the flexible hinge at T730–A731 affect the proton translocation properties of the sMTM7 region of the V_O domain? The second helical region of peptide sMTM7, which contains arginine 735, needs to be positioned in the centre of the membrane bilayer, thereby facing the central glutamic acids of the rotor (located at TM2 and TM4). As a consequence, the first helical region of sMTM7 is located in the cytoplasmic proton hemi-channel, in agreement with the bafilomycin binding data [7] (see Fig. 7). The flexible region of TM7 (i.e., T730–A731) that connects two helical segments thus is located near the end of the cytoplasmic hemi-channel (i.e. almost in the centre of the bilayer) (see Fig. 7). As region A738–Q745 does not fray in the extended version MTM7 of sMTM7 and as it has been shown to be helical in TM7 [5], this region is depicted as an helix in Fig. 7. We speculate that this proposed arrangement of the peptide in the hemi-channel could allow movement of protons to the centre of the rotor via rotation and adjustment of the first helical segment, thereby opening and closing the passage for protons to the centre of the membrane respectively (see blue arrows in Fig. 7). This movement could allow the correct orientation of the helical faces expected to be face-to-face during the different steps of proton translocation. Previously, Kawasaki-Nishi et al. [12] proposed that TM7 is a rigid helix and that changes in the orientation of TM4/TM2 relative to TM7 explain the experimental cross-links identified between TM7 and TM4/TM2. However, when TM7 consists of two helical segments that can rotate independently from one another, as we suggest, also explains the experimental cross-links observed between TM7 and TM4/TM2. Residues T730 and A731 can act as a dynamical ball-and-socket joint, which links two helical segments of sMTM7 in TM7. We propose that the autonomous movement of the N-terminal helical segment, which is positioned in the cytoplasmic hemi-channel, causes the proton translocation channel to open and close thereby enabling proton translocation (see blue arrows in Fig. 7).

The autonomous movement of the first helical segment of TM7 could also be relevant for the binding of inhibitors to specific amino acid residues of F- and V-ATPases (Fig. 1). Since the cytoplasmic loop that connects TM7 to TM6 is quite long (approximately 65 residues) dynamic movement of helix 1 of TM7 could be compensated by a movement further up in this loop. The existence of such a movement opens new opportunities for drug design. Inhibitors that bind to the cytoplasmic loop segment could rigidify it and thereby potentially disable the translocation of protons.

Acknowledgements

This work was supported by contract no. QLG-CT-2000-01801 of the European Commission (MIVase—New Therapeutic Approaches to Osteoporosis: targeting the osteoclast V-ATPase). The NMR spectra were recorded at the SON NMR Large Scale Facility in Utrecht, which is funded by the "Access to Research Infrastructures" program of the European Union (HPRI-CT-2001-00172).

Appendix A. Supplementary data

Supplementary data associated with this article can be found, in the online version, at doi:10.1016/j.bbamem.2007.05.014.

Fig. 7. Proposed model for opening and closing of the cytoplasmic hemi-channel of V_O-H^+-ATPase. Subunit *c* is represented by the rotor of Na^+-V-ATPase [4] (PDB entry: 2BL2). From subunit *a* only the section of TM7 that includes peptide sMTM7 is shown. The membrane boundaries (white horizontal lines) are according to Ref. [4]. Peptide sMTM7 is depicted as an α-helix with the exception of residues T730 and A731, which are highlighted by a white arrow and which form a flexible region that can allow Helix 1 and Helix 2 to move independently with respect to one another. The glutamic acids that are located in the rotor and R735 of peptide sMTM7 (depicted as a stick model) are colored red, while the other hydrophilic residues are colored in white. Hydrophobic residues are colored orange. Potential movements of TM7, based on the work presented here, that allow the cytoplasmic hemi-channel to "close" (A) or "open" (B) are indicated by blue arrows. The structures are drawn with the software package Chimera [33].

References

[1] M. Sambade, P.M. Kane, The yeast vacuolar proton-translocating ATPase contains a subunit homologous to the *Manduca sexta* and bovine e subunits that is essential for function, J. Biol. Chem. 279 (2004) 17361–17365.

[2] T. Nishi, M. Forgac, The vacuolar (H^+)-ATPases — nature's most versatile proton pumps, Nat. Rev., Mol. Cell Biol. 3 (2002) 94–103.

[3] K.W. Beyenbach, H. Wieczorek, The V-type H^+-ATPase: molecular structure and function, physiological roles and regulation, J. Exp. Biol. 209 (2006) 577–589.

[4] T. Murata, I. Yamato, Y. Kakinuma, A.G.W. Leslie, J.E. Walker, Structure of the rotor of the V-type Na^+-ATPase from *Enterococcus hirae*, Science 308 (2005) 654–659.

[5] A.M.S. Duarte, C.J.A.M. Wolfs, N.A.J. Van Nul, M.A. Harrison, J.B.C. Findlay, C.P.M. Van Mierlo, M.A. Hemminga, Structure and localization of an essential transmembrane segment of the proton translocation channel of yeast H^+-V-ATPase, Biochim. Biophys. Acta (2007) 218–227.

[6] W. Vos, L. Vermeer, M.A. Hemminga, Conformation of a peptide encompassing the proton translocation channel of vacuolar H^+-ATPase, Biophys. J. 92 (2007) 138–146.

[7] Y. Wang, T. Inoue, M. Forgac, Subunit a of the yeast V-ATPase participates in binding of bafilomycin, J. Biol. Chem. 280 (2005) 40481–40488.

[8] S. Kawasaki-Nishi, T. Nish, M. Forgac, Arg-735 of the 100-kDa subunit a of the yeast V-ATPase is essential for proton translocation, Proc. Natl. Acad. Sci. U. S. A. 98 (2001) 12397–12402.

[9] S. Kawasaki-Nishi, M. Forgac, Proton translocation driven by ATP hydrolysis in V-APTases, FEBS Lett. 555 (2003) 76–85.

[10] T. Nishi, S. Kawasaki Nishi, M. Forgac, The first putative transmembrane segment of subunit c″ (Vma16p) of the yeast V-ATPase is not necessary for function, J. Biol. Chem. 278 (2003) 5821–5827.

[11] M. Grabe, H.Y. Wang, G. Oster, The mechanochemistry of V-ATPase proton pumps, Biophys. J. 78 (2000) 2798–2813.

[12] S. Kawasaki-Nishi, T. Nishi, M. Forgac, Interacting helical surfaces of the transmembrane segments of subunits a and c′ of the yeast V-ATPase defined by disulfide-mediated cross-linking, J. Biol. Chem. 278 (2003) 41908–41913.

[13] Y. Wang, T. Inoue, M. Forgac, TM2 but not TM4 of subunit c″ interacts with TM7 of subunit a of the yeast V-ATPase as defined by disulfide-mediated cross-linking, J. Biol. Chem. 279 (2004) 44628–44638.

[14] J. Cavanagh, W.J. Fairbrother, A.J. Palmer III, N.J. Skelton, Protein NMR spectroscopy. Principles and practice, Academic Press, 1996.

[15] A.T. Brunger, P.D. Adams, G.M. Clore, W.L. DeLano, P. Gros, R.W. Grosse-Kunstleve, J.S. Jiang, J. Kuszewski, N. Nilges, N.S. Pannu, R.J. Read, L.M. Rice, T. Simonson, G.L. Warren, Crystallography and NMR system (CNS): a new software system for macromolecular structure determination, Acta Crystallogr. D54 (1998) 905–921.

[16] J. Linge, PhD thesis, Ruhr-Universitat Bochum, Bochum 2000.

[17] M. Nilges, S.I. O'Donoghue, Ambiguous NOEs and automated NOE assignment, Prog. Nucl. Magn. Reson. Spectrosc. 32 (1998) 107–139.

[18] R. Koradi, M. Billeter, K. Wüthrich, MOLMOL: a program for display and analysis of macromolecular structures, J. Mol. Graph. 14 (1996) 51–55.

[19] K. Wüthrich, NMR in biological research: peptides and proteins, North-Holland/American Elsevier, Amsterdam, 1976.

[20] K. Wüthrich, NMR of proteins and nucleic acids, Wiley, Amsterdam, NY, 1986.

[21] S. Deepak, R. Krishna, ^{13}C NMR chemical shifts can predict disulfide bond formation, J. Biomol. NMR V18 (2000) 165–171.

[22] C.C. Wang, J.H. Chen, S.H. Yin, W.J. Chuang, Predicting the redox state and secondary structure of cysteine residues in proteins using NMR chemical shifts, Proteins 63 (2006) 219–226.

[23] D.S. Wishart, B.D. Sykes, Chemical shifts as a tool for structure determination, Methods Enzymol. 239 (1994) 363–392.

[24] R.W. Hesselink, R.B.M. Koehorst, P.V. Nazarov, M.A. Hemminga, Membrane-bound peptides mimicking transmembrane Vph1p helix 7 of yeast V-ATPase: a spectroscopic and polarity mismatch study, Biochim. Biophys. Acta 1716 (2005) 137–145.

[25] P.L. Yeagle, G. Choi, A.D. Albert, Studies on the structure of the G-protein-coupled receptor rhodopsin including the putative G-protein binding site in unactivated and activated forms, Biochemistry 40 (2001) 11932–11937.

[26] P.L. Yeagle, C. Danis, G. Choi, J.L. Alderfer, A.D. Albert, Three dimensional structure of the seventh transmembrane helical domain of the G-protein receptor, rhodopsin, Mol. Vis. 27 (2000) 6125–6131.

[27] M. Bellanda, E. Peggion, R. Burgi, W. van Gunsteren, S. Mammi, Conformational study of an Aib-rich peptide in DMSO by NMR, J. Pept. Res. 57 (2001) 97–106.

[28] A. Motta, P.A. Temussi, E. Wunsch, G. Bovermann, A ^1H NMR study of human calcitonin in solution, Biochemistry 30 (1991) 2364–2371.

[29] S.M. Miick, K.M. Casteel, G.L. Millhauser, Experimental molecular dynamics of an alanine-based helical peptide determined by spin label electron spin resonance, Biochemistry 32 (1993) 8014–8021.

[30] B.K. Ho, A. Thomas, R. Brasseur, Revisiting the Ramachandran plot: hard-sphere repulsion, electrostatics, and H-bonding in the α-helix, Protein Sci. 12 (2003) 2508–2522.

[31] J. Underhaug, L.O. Jakobsen, M. Esmann, A. Malmendal, N.C. Nielsen, NMR studies of the fifth transmembrane segment of Na^+,K^+-ATPase reveals a non-helical ion-binding region, FEBS Lett. 580 (2006) 4777–4783.

[32] C. Hunte, E. Screpanti, M. Venturi, A. Rimon, E. Padan, H. Michel, Structure of a Na^+/H^+ antiporter and insights into mechanism of action and regulation by pH, Nature 435 (2005) 1197–1202.

[33] E.F. Pettersen, T.D. Goddard, C.C. Huang, G.S. Couch, D.M. Greenblatt, E. C. Meng, T.E. Ferrin, UCSF Chimera—a visualization system for exploratory research and analysis, J. Comput. Chem. 25 (2004) 1605–1612.